

General Formulas of Effective Earth Radius and Modified Refractive Index

GUOXU FENG¹, JUN HUANG, AND MINGXU YI

School of Aeronautic Science and Engineering, Beihang University, Beijing 100191, China

Corresponding author: Guoxu Feng (fengguoxu007@126.com)

This work was supported in part by Beihang University under Grant KH54210201 and Grant KZ01005001.

ABSTRACT The effective earth radius can transform the curved ray path into a straight line, and the modified refractive index can transform the spherical ground into a plane. Using them can simplify the propagation modeling of electromagnetic waves in the atmosphere, so they are widely used in the calculation of long-range propagation of electromagnetic wave, and adopted by the ITU Recommendations and the IEEE Standards. In this paper, upon employing simple geometric methods, we provide general formulas for the effective earth radius and the modified refractive index, pointing out that they both originate from the use of conformal transformations. In turn, we prove that for both quantities the formulas contained in the ITU Recommendations and the IEEE Standards are special cases of the general formulas given in this paper. Our results provide a solid mathematical background to the concepts of effective earth radius and modified refractive index, and pave the way for their use beyond the propagation of electromagnetic waves in the earth atmosphere, e.g. to the propagation of other types of waves in generic media.

INDEX TERMS Effective earth radius, modified refractive index, conformal transformation, wave propagation, ray tracing.

I. INTRODUCTION

The modeling of electromagnetic wave propagation in the atmosphere is at the basis of several engineering applications such as wireless communication [1]–[3], broadcasting [4], [5], navigation positioning [6], [7], and radar detection [8], [9]. Since atmospheric parameters such as pressure, temperature and humidity vary over time and space, so does the refractive index of the atmosphere [10]. In turn, the refractive index $n(t, \vec{r})$ of the atmosphere is a function of time t and space position \vec{r} . On the surface of the earth, n varies between 1.000250 and 1.000400, and decreases with the altitude [11]. In order to describe the change of n with time and space more easily, the atmospheric refractivity N is introduced, according to Eq. (1) [10], [11].

$$N = (n - 1) \times 10^6 \quad (1)$$

On the other hand, using long-term observations of atmospheric parameters around the world, the atmospheric refractivity may be summarized by the empirical formula

The associate editor coordinating the review of this manuscript and approving it for publication was Gerardo Di Martino¹.

shown in Eq. (2) [10], [11].

$$N = 77.6 \frac{p}{T} + 3.73 \times 10^5 \frac{e}{T^2}, \quad (2)$$

where p is the total atmospheric pressure in millibars, e is the water-vapor pressure in millibars, and T is the absolute atmospheric temperature in Kelvin.

Since $|\partial n / \partial t| \ll \|\nabla n\|$, we may safely assume that during the propagation of electromagnetic waves, n is just a function of \vec{r} . Where ∇ is gradient operator. Given the refraction index, the propagation path of electromagnetic wave may be obtained by solving the eikonal equation [12].

$$\|\nabla \phi\| = n. \quad (3)$$

where ∇ is wave front. Whereas the electric field is obtained by solving the Helmholtz equation [13].

$$\left(\nabla^2 + k_0^2 n^2\right) \Psi = 0 \quad (4)$$

where Ψ is a scalar potential and k_0 is the wavenumber in vacuum.

The nonuniform nature of the atmospheric refractive index and the existence of the curvature of the earth make it difficult to solve these two equations directly. In order to make the problem easier, the concepts of *effective earth radius*

(EER) [14] and *modified refractive index* (MRI) [15] have been put forward. The concept of EER is used to transform the curved path of electromagnetic wave near the earth's surface into an equivalent straight line, whereas using MRI, one may approximately eliminate the curvature of the earth.

Although the concepts of EER and MRI has gained widespread application and has been adopted in several ITU Recommendations [1], [10], [16]–[20], no simple and rigorous mathematical derivation has been provided so far. At variance with previous proposals, in this paper, we derive the general formulas for EER and MRI by exploiting simple geometric methods, pointing out that they both originate from the use of conformal transformations, and prove that for both quantities the formulas contained in the ITU Recommendations and the IEEE Standards are special cases of the general formulas given here. We believe that our work may provide a useful reference to address electromagnetic wave propagation in the atmosphere.

The content of this paper is arranged as follows: Section 1 provides a general background, introducing the concepts of propagation prediction, modified refractive index, EER and MRI. Section 2 consists of a brief review of research about EER and MRI, and points out that formulas that may be found in literature are approximate ones. In sections 3 and 4, general formulas for EER and MRI are given and discussed by a simple geometric approach. Section 5 closes the paper with some concluding remarks.

II. HISTORICAL REVIEW

A. EFFECTIVE EARTH RADIUS

The concept of EER was proposed by Schelling, Burrows and Ferrell of Bell Telephone Laboratories in 1933, in the study the ultrashort wave propagation near the earth's surface [14]. They assumed that the atmospheric refractive index is a spherical layered distribution and decreased linearly with increasing altitude. Then, the approximate expression of EER may be obtained according to the principle of *curvature difference invariance*. The use of EER makes it easy to calculate the propagation effects of electromagnetic wave near the earth's surface, such as refraction [16], diffraction [17], electromagnetic interference [18], and rain attenuation [19].

Under the small angle approximation, Miller gave an approximate expression for EER by using the principle of curvature difference invariance [21]. Freehafer *et al.* [22] derived an approximate relationship between EER and MRI, and used MRI to indirectly obtain approximate expression for EER, but did not give a direct derivation method for the EER. Robertshaw [23] used the ray tracing method to give a practical interpolation table for calculating the EER factor at altitudes larger than 1 km. In the small angle approximation, Doviak and Zrnica [24] derived the approximate expression of EER by using the ray differential equation of electromagnetic wave propagation. Palmer and Baker [25]

proposed a semi empirical model to calculate the EER factor based on the observed data. Craig [26] used the principle of curvature difference invariance to give an approximate expression for the EER under the condition of low elevation angle.

B. MODIFIED REFRACTIVE INDEX

The concept of MRI was first proposed by Pryce, and then published by Pekeris [15]. In that paper, Pekeris used MRI to convert the earth's spherical ground into a plane ground, and provided the asymptotic solutions for the normal modes of Helmholtz equation. Similar to the refractivity N in Eq. (1), the refractive modulus M is defined using the MRI m as $M = (m - 1) \times 10^6$ [20]. The vertical gradient of this quantity, i.e. dM/dh is used to characterize the type of atmospheric refraction [27].

In the same year 1946, Leontovich and Fock simplified Helmholtz equation deriving a more easily solved parabolic equation using paraxial approximation, and studied the propagation of electromagnetic waves near the earth's surface [28]. Due to limited computational power at the time, the parabolic equation approximation did not attract much attention for a long period [29]. However, in 1972, Hardin and Tappert proposed a split-step Fourier method that could use computers to solve parabolic equations efficiently and deal with underwater acoustic propagation problems [30]. Since then, the parabolic equation method has been widely studied, and various numerical solutions algorithms have emerged [29], [31].

At present, the parabolic equation method has become a very important tool to approximately solve problems in electromagnetic wave propagation. In this framework, the MRI m is a key parameter since it allows one to transform the spherical atmosphere into a cuboid, thus ensuring that the paraxial approximation is not limited by the propagation distance [32]. In problems involving electromagnetic wave propagation, it is common to use the following two-dimensional parabolic equation [32] in the vertical plane $x - h$,

$$\frac{\partial^2 u}{\partial x^2} + 2ik_0 \frac{\partial u}{\partial x} + \frac{\partial^2 u}{\partial h^2} + k_0^2 (m^2 - 1) u = 0, \quad (5)$$

where, $u(x, h) = e^{-ik_0 x} \Psi(x, h)$.

Pekeris [15] suggested an approximated expression for the MRI (without proof), and then put forward a relationship between the MRI and the EER by ignoring high-order terms. By simple comparison of Snell's and Bouguer's law, Freehafer *et al.* obtained an approximating formula for the MRI, however following a method not fully rigorous [22]. The formula of MRI reported in ITU-R P.310-10 Recommendation [20] and IEEE Standards [33]–[36] can be obtained by this approximating formula. Since this formula has been included in the standard document for more than 50 years, researchers tend to adopt it without proof [26], [27], [32].

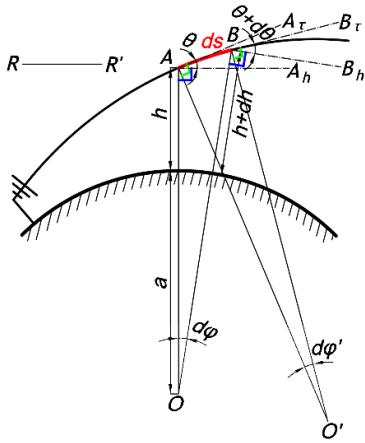


FIGURE 1. Schematic diagram of electromagnetic wave propagation in the atmosphere.

III. EFFECTIVE EARTH RADIUS
A. FORMULA DERIVATION

Fig. 1 is a schematic diagram of electromagnetic wave propagation in the atmosphere: ds is the infinitesimal path of the electromagnetic wave, with starting and ending point denoted by A and B , respectively, AA_τ and BB_τ are the lines tangent to the wave path at points A and B , whereas AA_h and BB_h are horizontal lines at points A and B . The points A and B are at altitudes h and $h + dh$, whereas θ and $\theta + d\theta$ denote the elevation angles of the two points with respect to the horizontal line at points A and B respectively. Finally, O is the center of the earth, O' is the center of curvature for the infinitesimal path and RR' is the reference line segment for rotations, i.e. angles are positive (negative) when they denote counterclockwise (clockwise) rotation with respect to RR' .

According to the above assumptions, the following angle relations may be obtained from Fig. 1.

$$\theta = AA_\tau - AA_h, \tag{6a}$$

$$\theta + d\theta = BB_\tau - BB_h, \tag{6b}$$

$$d\varphi = AA_h - BB_h, \tag{6c}$$

$$d\varphi' = AA_\tau - BB_\tau, \tag{6d}$$

and therefore,

$$d\varphi' = d\varphi - d\theta. \tag{7}$$

The relationship between the length of the wave path ds and the difference in altitude dh between the extremal points A and B is given by

$$ds = \frac{dh}{\sin \theta}, \tag{8}$$

whereas the curvature C_k of the infinitesimal path may be obtained from Eqs. (7) and (8),

$$C_k = \frac{d\varphi'}{ds} = \frac{\cos \theta}{a+h} - \sin \theta \frac{d\theta}{dh}, \tag{9}$$

where a is the average earth radius.

If $C_k = 0$, electromagnetic waves propagate on a straight line and the following linear equation may be obtained

$$\frac{d\theta}{dh} = \frac{\cot \theta}{a+h}, \tag{10}$$

Eq. (10) is a linear equation in the coordinate system $(h, \theta) |_{\infty}$. Since a ray may be seen as circle with curvature radius $a = \infty$, we may look at $(h, \theta) |_{\infty}$ as an extended polar coordinate system.

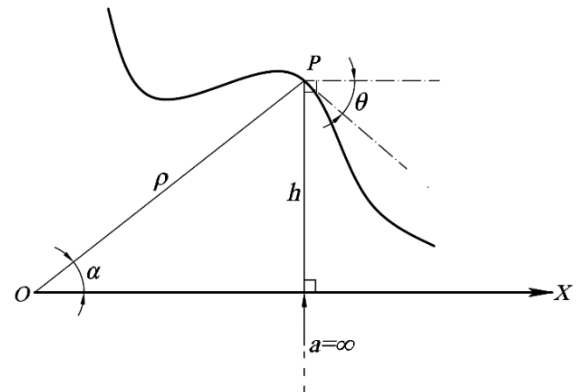


FIGURE 2. Schematic diagram of the relationship between polar coordinate system (ρ, α) and $(h, \theta) |_{\infty}$ coordinate system.

As shown in Fig. 2, the ray OX is used as a reference curve, and polar coordinates (ρ, α) are employed to describe any point P on the curve. According to the geometry of the system, we obtain the expressions of h and θ expressed by ρ and α as shown in Eq. (11).

$$h = \rho \sin \alpha, \tag{11a}$$

$$\theta = \arctan \left(\frac{\frac{d\rho}{d\alpha} \sin \alpha + \rho \cos \alpha}{\frac{d\rho}{d\alpha} \cos \alpha - \rho \sin \alpha} \right). \tag{11b}$$

Eq. (11) shows that (h, θ) and (ρ, α) are linked to each other. Both of them use the OX axis as a reference curve to describe the parameter group of the point P , that is, the $(h, \theta) |_{\infty}$ coordinate system and the polar coordinate system (ρ, α) are equivalent. Therefore, it can be considered that the coordinate system $(h, \theta) |_{\infty}$ defined in this article is a generalization of the polar coordinate system.

Assuming that the refractive index n of the atmosphere is only function of the altitude h , a condition usually referred to as *horizontal uniform spherical stratification condition*, the propagation of electromagnetic waves satisfies the so-called Bouguer's law [37], i.e.

$$n(a+h) \cos \theta = \text{const} \tag{12}$$

By differentiating Eq. (12) with respect to h , we obtain

$$\frac{dn}{dh} (a+h) \cos \theta + n \cos \theta - n(a+h) \sin \theta \frac{d\theta}{dh} = 0, \tag{13}$$

which may be rewritten as

$$\frac{d\theta}{dh} = \left(\frac{1}{n} \frac{dn}{dh} + \frac{1}{a+h} \right) \cot \theta. \tag{14}$$

Eq. (14) is defined in the coordinate system $(h, \theta)|_{\odot a}$. If $dn/dh = 0$, Eq. (14) collapses to Eq. (10). If an EER a_e is defined according to Eq. (15), then Eq. (14) can be converted into Eq. (16), which reproduces the functional form of Eq. (10).

$$\frac{1}{a_e + h} = \frac{1}{n} \frac{dn}{dh} + \frac{1}{a + h}, \quad (15)$$

$$\frac{d\theta}{dh} = \frac{\cot \theta}{a_e + h}. \quad (16)$$

Eq. (16) is a linear equation defined in coordinate system $(h, \theta)|_{\odot a_e}$. Moving from Eqs. (14) to (16) amounts to a coordinate transformation, which is given by Eq. (15). The transformation leaves the values of h and θ unchanged, while it reshapes the wave path from a curve to a straight line, thus simplifying the path calculation problem. Fig. 3 shows a schematic diagram illustrating the use of the EER a_e to realize coordinate transformation.

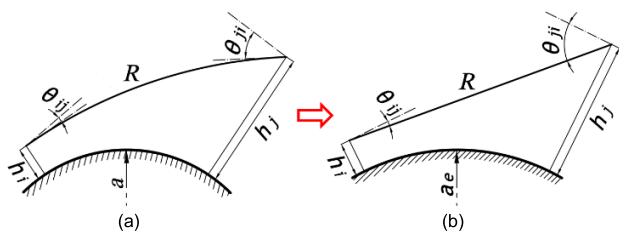


FIGURE 3. Principle of effective earth radius. (a) Coordinate system $(h, \theta)|_a$. (b) Coordinate system $(h, \theta)|_{\odot a_e}$.

It is not difficult to see that the angle between two paths is preserved by the Eq. (15), which therefore describes a conformal transformation [38]. According to Eq. (15), the general expression for the EER a_e is given by

$$a_e = (a + h) \left(1 + \frac{(a + h)}{n} \frac{dn}{dh} \right)^{-1} - h. \quad (17)$$

The modification induced by Eq. (15) are often quantified by the EER factor $k = a_e/a$, which according to Eq. (17), may be written as

$$k = \frac{a + h}{a} \left(1 + \frac{(a + h)}{n} \frac{dn}{dh} \right)^{-1} \frac{h}{a}. \quad (18)$$

At low altitudes, i.e. if $h \ll a$, Eq. (17) may be further simplified to

$$a_e \approx \left(\frac{1}{a} + \frac{1}{n} \frac{dn}{dh} \right)^{-1}. \quad (19)$$

Let $a + h = r$, $dh = dr$ can be obtained. By substituting it into Eq. (19), we obtain Eq. (20), which is exactly the approximate expression of EER given by Miller [21].

$$a_e \approx \left(\frac{1}{a} + \frac{1}{n} \frac{dn}{dr} \right)^{-1}. \quad (20)$$

For the earth's atmosphere, since the refractive index $n \approx 1$ [10], [11], Eq. (19) can be further approximated by Eq. (21),

which coincides with the approximate expression of EER given by Doviak and Zrnica [24], and Craig [26].

$$a_e \approx \left(\frac{1}{a} + \frac{dn}{dr} \right)^{-1}. \quad (21)$$

Correspondingly, the EER factor k may be written as

$$k \approx \left(1 + a \frac{dn}{dh} \right)^{-1}. \quad (22)$$

Eqs. (21) and (22) are the standard definitions of a_e and k given in ITU-R P.310-10 Recommendations [20]. The average earth radius is given by $a = 6371230\text{m}$ [39], for the atmosphere in standard conditions and at zero altitude, the average value of dn/dh is $-39.232 \times 10^{-6}/\text{km}$ [40]. Upon substituting these values into Eq. (22), we arrive at $k = 1.3333 \approx 4/3$, which corresponds to the celebrated 4/3 earth radius model [20].

B. DISCUSSION

Although the concept of EER has been introduced on the assumption that the earth's atmosphere satisfies the horizontal uniform spherical stratification condition, its validity extends to situations where the condition is not strictly satisfied. If the length s of the electromagnetic wave ray path is taken as an independent variable, the altitude h and the refractive index n are both functions of s , so that Eq. (17) can be rewritten into the form of Eq. (23).

$$a_e(s) = (a + h(s)) \left(1 + \frac{a + h(s)}{n(s)} \frac{\dot{n}(s)}{\dot{h}(s)} \right)^{-1} - h(s), \quad (23)$$

where $\dot{n}(s) = dn/ds$ and $\dot{h}(s) = dh/ds$.

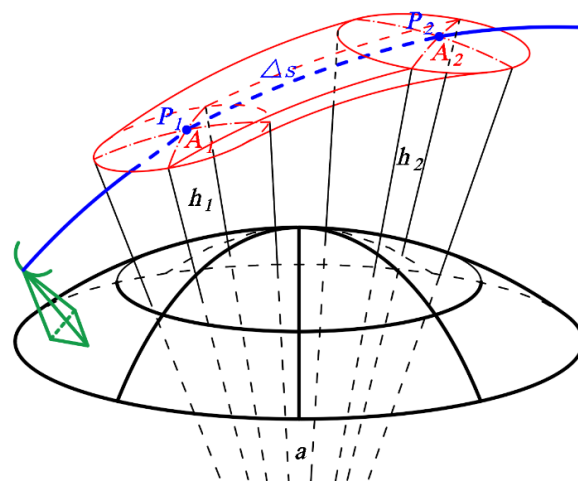


FIGURE 4. Schematic diagram of the tubular region satisfying the horizontal uniform spherical stratification condition on the electromagnetic wave propagation path.

Because EER a_e is a univariate function of s , the concept of EER is valid as long as the atmospheric refractive index satisfies the horizontal uniform spherical stratification condition in the tubular region containing ray the paths. This is illustrated in Fig. 4. In the figure, P_1 and P_2 are two points

on the ray path with a distance of Δs , and their altitudes are h_1 and h_2 respectively, A_1 and A_2 are the areas of local horizontal planes at points P_1 and P_2 respectively.

In most cases, the change rate of atmospheric refractive index in the horizontal plane is much lower than that in the vertical plane [10], [11]. Therefore, the EER method is effective as long as there are no strong convective phenomena along the ray path, which in turn may destroy the stratification state of refractive index in the tubular region.

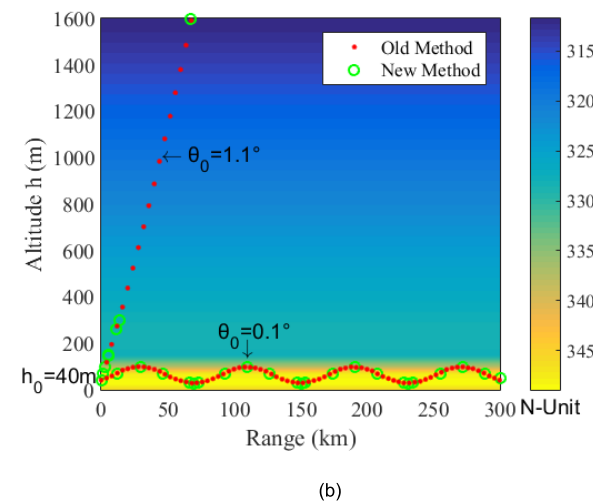
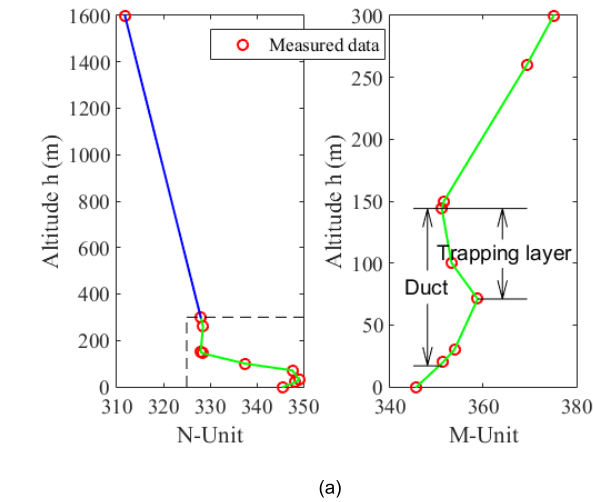


FIGURE 5. Ray tracing comparison chart based on measured data. (a) Radiosonde measurement data. (b) Comparison of two ray tracing methods.

Fig. 5 (a) is the variation curve of refractivity N and refractive modulus M with altitude h obtained from radiosonde measurement data [41]. There are 10 data points in the figure. According to the $M-h$ curve, the altitude range of the duct layer and the trapping layer can be obtained [41]. Substituting those 10 data points into Eq. (17) one may obtain the EER in the 9 altitude layers. Given the altitude h_0 and elevation angle θ_0 of the transmitting antenna, and using these EERs, the electromagnetic ray path tracking can be realized.

Fig. 5 (b) shows the comparison of the two ray tracing methods. The red dots in the figure are the results obtained by the ray differential equation method of [41], and the green circles are the results obtained by the piecewise EER method. The two methods are in good agreement, but the latter only needs a few data points, and only needs algebraic operation, so there is no numerical stability problem. When $\theta_0 = 1.1^\circ$, the electromagnetic wave is standard propagation, and the piecewise EER method only needs to calculate 9 points to achieve ray tracing. When $\theta_0 = 0.1^\circ$, electromagnetic waves will be captured by the trapping layer and propagate in the duct. According to the periodicity of propagation path, only 5 points need to be calculated to realize ray tracing. It can be seen that when there is only one refractivity profile, that is, the horizontal uniform spherical stratification atmosphere, the electromagnetic wave propagation path can be obtained very conveniently and quickly by using the piecewise EER method. However, the approximate formula of EER cannot deal with electromagnetic wave propagation in atmospheric duct.

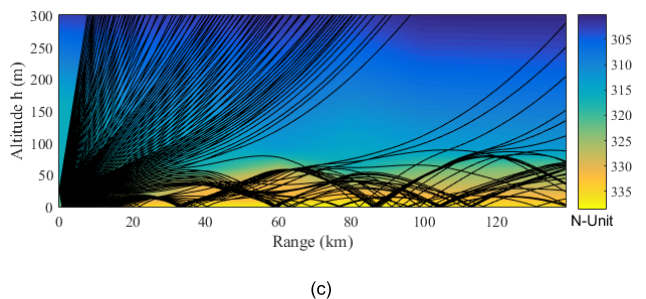
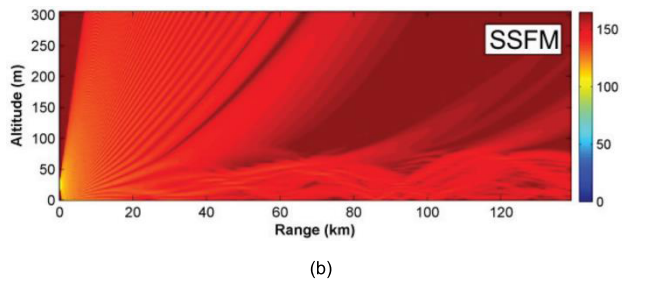
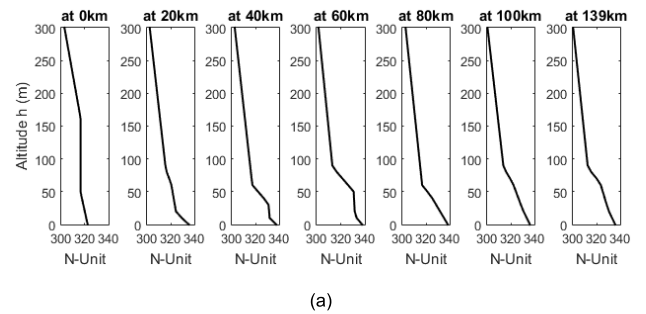


FIGURE 6. Ray tracing comparison chart in non-uniform atmosphere. (a) Refractivity profiles. (b) Propagation pathloss (dB) by using SSFM. (c) Ray tracing by using piecewise EER.

If there are multiple refractivity profiles along the propagation path of electromagnetic wave, i.e. non-uniform atmosphere, the ray tracing can also be easily realized by

using the piecewise EER method to compile a computer program. Fig. 6 (a) shows seven refractivity profiles of non-uniform atmosphere given in reference [42]. Fig. 6(b) shows the propagation pathloss distribution obtained by solving parabolic equation with split-step Fourier transform method (SSFm) in reference [42]. Fig. 6 (c) shows the ray tracing curve obtained by using the piecewise EER method. The altitude of the antenna is $h_0 = 26\text{m}$, and the beam width is 2° [42].

Although the calculation contents illustrated in Fig. 6(b) and Fig. 6(c) are different, their trends are consistent. The larger the ray density is, the smaller the propagation pathloss is. Fig. 6 shows that the piecewise EER method can be used to realize ray tracing in non-uniform atmospheric conditions. However, the approximate formula of EER cannot deal with electromagnetic wave propagation in non-uniform atmosphere.

To sum up, the general formula of EER given here overcomes the limitations of approximate formulas and largely expands the potential use of EER. In addition, it is easy to see from our derivations that Eqs. (21) and (22) may be used only for the propagation of electromagnetic wave in the atmosphere near the earth's surface (i.e. $n \approx 1$ and $h \ll a$). On the other hand, Eqs. (17) and (18) have no restrictions, i.e. they are neither limited to electromagnetic wave nor to specific types of medium. Eqs. (17) and (18) may be thus used to evaluate exactly the propagation path of any type of wave in any spherical layered medium.

In optics, Maxwell fish-eye lenses [43], Luneburg lenses [44], Eaton lenses [45] and invisible lenses [43] are all spherical layered media. In astronomy, planetary atmospheres involved in ground-based astro-geodetic observations and atmospheric occultations observations are often modeled as spherical stratified media [46]. In marine acoustics, the underwater sound velocity profile is often modeled as spherical layered media, based on which the acoustic path is calculated [47]. In seismology, the crustal structure in the calculation of seismic waves travel time is often modeled as a spherical layered structure [48]. The general formula of EER given here can be a useful tool in all these fields.

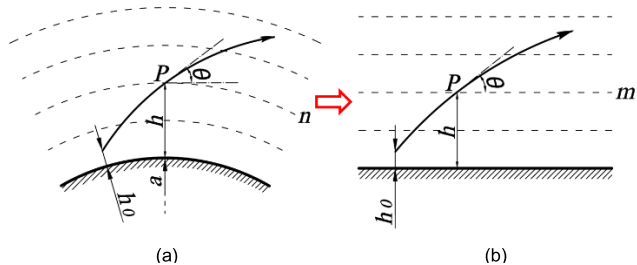


FIGURE 7. Principle of modified refractive index. (a) Spherically stratified atmosphere. (b) Planarly stratified atmosphere.

IV. MODIFIED REFRACTIVE INDEX
A. FORMULA DERIVATION

In Fig. 7 we illustrate the use of MRI concept to transform a spherically stratified atmosphere into an equivalent planarly

stratified atmosphere. The MRI is a relevant tool for determining the propagation of electromagnetic waves, since the parabolic equation method, which is widely used in this context, takes the modified refractive index m as the basic input parameter [32].

In order to exactly evaluate the MRI, let us start from the well known Snell's law for the propagation of electromagnetic wave in planarly stratified medium, i.e.

$$m \cos \theta = \text{const.} \tag{24}$$

By differentiating Eq. (24) with respect to h , we have

$$\frac{dm}{dh} \cos \theta - m \sin \theta \frac{d\theta}{dh} = 0 \tag{25}$$

and, in turn,

$$\frac{d\theta}{dh} = \frac{1}{m} \frac{dm}{dh} \cot \theta. \tag{26}$$

The electromagnetic wave propagation in a spherical layered medium satisfies Bouguer's law as shown in Eq. (12), that is, satisfies the differential equation as shown in Eq. (14). It is not difficult to see that Eqs. (14) and (26) describe the same electromagnetic wave propagation path. Similar to the EER, the transformation from Eqs. (14) to (26) using the MRI is also a conformal transformation [38]. The former uses a_e to transform the curved path into a straight line, and the object of transformation is the shape of the electromagnetic wave propagation path; the latter uses m to transform the spherical stratified atmosphere into a plane, and the object of transformation is the shape of the atmospheric medium. Although they have different transformation objects, their mathematical principles are identical.

From Eqs. (14) and (26), we arrive at the transformation

$$\frac{1}{m} \frac{dm}{dh} = \frac{1}{n} \frac{dn}{dh} + \frac{1}{a+h}. \tag{27}$$

Which allows us find an analytic expression for m . To this aim we notice that the radius of earth is a constant and the above equation may be rewritten as

$$\frac{1}{m} \frac{dm}{d(a+h)} = \frac{1}{n} \frac{dn}{d(a+h)} + \frac{1}{a+h}, \tag{28}$$

i.e.

$$\frac{1}{m} \frac{dm}{dr} = \frac{1}{n} \frac{dn}{dr} + \frac{1}{r}, \tag{29}$$

where we used $a+h = r$. We now use the imaginary compound function to represent,

$$m = \exp(F(r)), \tag{30}$$

which leads to

$$\frac{dm}{dr} = \exp(F(r)) \frac{dF(r)}{dr} = m \frac{dF(r)}{dr}. \tag{31}$$

Upon substituting Eq. (31) into Eq. (29) we have

$$\frac{dF(r)}{dr} = \frac{1}{n} \frac{dn}{dr} + \frac{1}{r}. \tag{32}$$

Integrating Eq. (32) we have

$$F(r) = \ln(Cnr), \tag{33}$$

where C an undetermined integral constant. Finally, we arrive at

$$m = Cnr. \tag{34}$$

Let us now focus attention to the infinitesimal region $\delta\Omega$, where the electromagnetic source is located. In this case, the path length δs is infinitesimal, that is, $\delta s/a \sim 0$ and the earth curvature is zero, i.e. the atmospheric refractive index in $\delta\Omega$ space is plane stratified. Let us denote by n_0 and m_0 the refraction index and modified refractive index in $\delta\Omega$, then the initial condition is

$$m_0 = n_0. \tag{35}$$

If the electromagnetic source is at altitude h_0 , then the constant C can be obtained by substituting Eq. (35) into Eq. (34).

$$C = \frac{1}{a + h_0} \tag{36}$$

By substituting Eq. (36) into Eq. (34), the expression of MRI m can be obtained as

$$m = \frac{a + h}{a + h_0} n. \tag{37}$$

If $h_0 \ll a$, then Eq. (37) can be approximated to Eq. (38), which is exactly the same as the formula given by Freehafer *et al.* [22].

$$m \approx \frac{a + h}{a} n = \left(1 + \frac{h}{a}\right) n \tag{38}$$

For the earth's atmosphere, the refractive index $n \approx 1$, so Eq. (38) can be further approximated to Eq. (39).

$$m \approx n + \frac{h}{a} \tag{39}$$

Eq. (39) is the formula of the MRI given in ITU-R P.310-10 Recommendation [20] and IEEE Standards [33]–[36].

For the sake of completeness, we also notice that the exact expression for the refractive modulus M can be given by using Eq. (37), arriving at

$$M = \left(\frac{a + h}{a + h_0} n - 1\right) \times 10^6. \tag{40}$$

B. DISCUSSION

It can be seen from Eq. (37) that the general expression of MRI m is a function of three variables: refractive index n , altitude h and source altitude h_0 , that is, $m(n, h, h_0)$. Eq. (38) can be expressed by $m(n, h, 0)$. So, the relative error ε of approximate formula for the MRI can be obtained as follows

$$\varepsilon \approx \frac{m(n, h, 0) - m(n, h, h_0)}{m(n, h, h_0)} = \frac{h_0}{a}. \tag{41}$$

The main purpose of the MRI m is to solve the parabolic equation. The advantage of parabolic equation method is

that it can directly give the distribution of electric field intensity, so as to uniformly calculate the propagation effect of interference and diffraction caused by the environment. The drawback is that the calculations are limited by the electric size of the calculation domain. Multi functional wave propagation calculation software generally needs to integrate a variety of different solvers [49], of which the parabolic equation method is mainly used to solve the wave propagation in the near surface airspace. Under the current computer hardware conditions, the practical problems that can be solved by using the parabolic equation method all satisfy $h_0 \ll a$, i.e. $\varepsilon \approx 0$. The refractive modulus M related to the MRI m is mainly used to determine the refraction type of the lower atmosphere, and it also satisfies $h_0 \ll a$.

It can be seen that for the current practical applications, the general formula of MRI is not superior to the approximate formula, and the difference between them is very small. On the other hand, with more powerful computers, the solution of parabolic equation will no longer be limited to the electric size of the calculation domain, and in that case the general formula of MRI will show its advantage. In addition, it can be seen from the derivation process that Eq. (39) is only applicable to the propagation of electromagnetic wave in the earth atmosphere and close to the surface ($n \approx 1$ and $h_0 \ll a$). On the other hand, Eq. (37) have no restrictions and may be used for any kind of wave in any kind of medium. Similar to the EER, the MRI also is derived from conformal transformation. In turn, this method of dealing with wave propagation may be useful also in more general contexts.

Finally, we emphasize that the expression in Eq. (37) coincides with the concept of composite refractive index introduced in [50] (notice the change in the name). There are two reasons for merging our present results with previous ones. On the one hand, MRI and EER are two basic concepts to deal with electromagnetic wave propagation in the atmosphere, both of which are derived from conformal transformation. However, the strong connections between them have not been emphasized in previous literature. Putting them together helps to fully show the similarities and differences between the two concepts. On the other hand, the MRI has been widely used in discussing radio propagation, but referring to it as composite refractive index made it difficult to attract attention from the relevant community.

V. CONCLUSION

Effective earth radius and modified refractive index are two relevant tools in the study of electromagnetic wave propagation in the earth atmosphere. Although their introduction is based on different principles, they are both based on conformal transformations. In this paper, the exact general forms of effective earth radius and modified refractive index have been obtained showing that their use is not limited to the propagation of electromagnetic waves in earth atmosphere. Rather, EER and MRI may be used to simplify the study of the propagation of any kind of wave in any kind of medium.

We have also explicitly shown that the formulas to evaluate the EER and the MRI given in the ITU Recommendations and IEEE Standards are special cases of the general formulas given in this paper. Our results clarify the meaning and the range of application of EER and MRI concepts and pave the way for their use in more general contexts.

ACKNOWLEDGMENT

The authors would like to express their gratitude to EditSprings (<https://www.editsprings.com/>) for the expert linguistic services provided.

REFERENCES

- [1] *Propagation Data and Prediction Methods Required for the Design of Earth-Space Telecommunication Systems*, document ITU-R P.618-13, Dec. 2017.
- [2] I. Bilal, A. Meijerink, and M. J. Bentum, "A frequency offset transmit reference system in dense multipath environments: Propagation effects and design considerations," *IEEE Trans. Wireless Commun.*, vol. 19, no. 2, pp. 859–873, Feb. 2020, doi: [10.1109/TWC.2019.2949783](https://doi.org/10.1109/TWC.2019.2949783).
- [3] A. I. Sulyman, A. Alwarafy, G. R. MacCartney, T. S. Rappaport, and A. Alsanie, "Directional radio propagation path loss models for millimeter-wave wireless networks in the 28-, 60-, and 73-GHz bands," *IEEE Trans. Wireless Commun.*, vol. 15, no. 10, pp. 6939–6947, Oct. 2016, doi: [10.1109/TWC.2016.2594067](https://doi.org/10.1109/TWC.2016.2594067).
- [4] I. Pena, T. Lauterbach, P. Angueira, A. Arrinda, J. M. Matias, D. de la Vega, M. M. Velez, C. Re, and F. Maier, "Planning factors for digital local broadcasting in the 26 MHz band," *IEEE Trans. Broadcast.*, vol. 57, no. 1, pp. 24–36, Mar. 2011, doi: [10.1109/TBC.2010.2100154](https://doi.org/10.1109/TBC.2010.2100154).
- [5] J. C. H. Wang, "Seasonal variation of LF/MF sky-wave field strengths," *IEEE Trans. Broadcast.*, vol. 54, no. 3, pp. 437–440, Sep. 2008, doi: [10.1109/TBC.2008.919390](https://doi.org/10.1109/TBC.2008.919390).
- [6] R. Norman, J. L. Marshall, W. Rohm, B. A. Carter, G. Kirchengast, S. Alexander, C. Liu, and K. Zhang, "Simulating the impact of refractive transverse gradients resulting from a severe troposphere weather event on GPS signal propagation," *IEEE J. Sel. Topics Appl. Earth Observ. Remote Sens.*, vol. 8, no. 1, pp. 418–424, Jan. 2015, doi: [10.1109/JSTARS.2014.2344091](https://doi.org/10.1109/JSTARS.2014.2344091).
- [7] D.-D. Wang, X.-L. Xi, Y.-R. Pu, J.-F. Liu, and L.-L. Zhou, "Parabolic equation method for Loran-C ASF prediction over irregular terrain," *IEEE Antennas Wireless Propag. Lett.*, vol. 15, pp. 734–737, 2016, doi: [10.1109/LAWP.2015.2471079](https://doi.org/10.1109/LAWP.2015.2471079).
- [8] L. Sevgi, "Modeling and simulation challenges in wide ocean area surveillance," *IEEE Access*, vol. 7, pp. 117692–117698, 2019, doi: [10.1109/ACCESS.2019.2924261](https://doi.org/10.1109/ACCESS.2019.2924261).
- [9] B. W. Dowd and R. E. Diaz, "FDTD simulation of very large domains applied to radar propagation over the ocean," *IEEE Trans. Antennas Propag.*, vol. 66, no. 10, pp. 5333–5348, Oct. 2018, doi: [10.1109/TAP.2018.2852141](https://doi.org/10.1109/TAP.2018.2852141).
- [10] *The Radio Refractive Index: Its Formula and Refractivity Data*, document ITU-R P.453-14, Aug. 2019.
- [11] W. L. Patterson, "The propagation factor, F_p , in the radar equation," in *Radar Handbook*, 3th ed. New York, NY, USA: McGraw-Hill, 2008, p. 263.
- [12] G. Feng and J. Huang, "A new method for solving the eikonal equation in the spherical computing domain," *Math. Methods Appl. Sci.*, vol. 43, no. 6, pp. 2953–2966, Jan. 2020, doi: [10.1002/mma.6093](https://doi.org/10.1002/mma.6093).
- [13] C. C. Constantinou, "Numerically intensive propagation prediction methods," in *Propagation of Radiowaves*, 2nd ed. London, U.K.: The Institution of Engineering and Technology, 2003, pp. 169–178.
- [14] J. C. Schelleng, C. R. Burrows, and E. B. Ferrell, "Ultra-short wave propagation," *Bell System Tech. J., The*, vol. 12, no. 2, pp. 125–161, Apr. 1933, doi: [10.1002/j.1538-7305.1933.tb03220.x](https://doi.org/10.1002/j.1538-7305.1933.tb03220.x).
- [15] C. L. Pekeris, "Asymptotic solutions for the normal modes in the theory of microwave propagation," *J. Appl. Phys.*, vol. 17, no. 12, pp. 1108–1124, Dec. 1946, doi: [10.1063/1.1707683](https://doi.org/10.1063/1.1707683).
- [16] *Effects of Tropospheric Refraction on Radiowave Propagation*, document ITU-R P.834-9, Dec. 2017.
- [17] *Propagation by Diffraction*, document ITU-R P.526-15, Oct. 2019.
- [18] *Prediction Procedure for the Evaluation of Interference Between Stations on the Surface of the Earth at Frequencies Above About 0.1 GHz*, document ITU-R P.452-16, Jul. 2015.
- [19] *Propagation Data and Prediction Methods Required for the Design of Terrestrial Line-of-Sight Systems*, document ITU-R P.530-17, Dec. 2017.
- [20] *Definitions of Terms Relating to Propagation in Non-Ionized Media*, document ITU-R P.310-10, Aug. 2019.
- [21] W. Miller, "Effective earth's radius for radiowave propagation beyond the horizon," *J. Appl. Phys.*, vol. 22, no. 1, pp. 55–62, Jan. 1951, doi: [10.1063/1.1699820](https://doi.org/10.1063/1.1699820).
- [22] J. E. Freehafer, W. T. Fishback, W. H. Furry, and D. E. Kerr, "Theory of propagation in a horizontally stratified atmosphere," in *Propagation of Short Radio Waves*. New York, NY, USA: McGraw-Hill, 1951, pp. 27–180.
- [23] G. A. Robertshaw, "Effective earth radius for refraction of radio waves at altitudes above 1 km," *IEEE Trans. Antennas Propag.*, vol. AP-34, no. 9, pp. 1099–1105, Sep. 1986, doi: [10.1109/TAP.1986.1143948](https://doi.org/10.1109/TAP.1986.1143948).
- [24] R. J. Doviak and D. S. Zrnic, "Electromagnetic waves and propagation," in *Doppler Radar and Weather Observations*, 2nd ed. London, U.K.: Academic, 1993, pp. 10–29.
- [25] A. J. Palmer and D. C. Baker, "A novel simple semi-empirical model for the effective earth radius factor," *IEEE Trans. Broadcast.*, vol. 52, no. 4, pp. 557–565, Dec. 2006, doi: [10.1109/TBC.2006.884737](https://doi.org/10.1109/TBC.2006.884737).
- [26] K. H. Craig, "Clear-air characteristics of the troposphere," in *Propagation of Radiowaves*, 2nd ed. London, U.K.: The Institution of Engineering and Technology, 2003, pp. 103–112.
- [27] E. Dinc and O. B. Akan, "Channel model for the surface ducts: Large-scale path-loss, delay spread, and AOA," *IEEE Trans. Antennas Propag.*, vol. 63, no. 6, pp. 2728–2738, Jun. 2015, doi: [10.1109/TAP.2015.2418788](https://doi.org/10.1109/TAP.2015.2418788).
- [28] M. Leontovich and V. Fock, "Solution of the problem of propagation of electromagnetic waves along the earth's surface by the method of parabolic equation," *Acad. Sci. USSR. J. Phys.*, vol. 10, pp. 13–24, 1946.
- [29] D. Lee, A. D. Pierce, and E.-C. Shang, "Parabolic equation development in the twentieth century," *J. Comput. Acoust.*, vol. 8, no. 4, pp. 527–637, Dec. 2000, doi: [10.1142/S0218396X00000388](https://doi.org/10.1142/S0218396X00000388).
- [30] R. H. Hardin and F. D. Tappert, "Application of the split-step Fourier method to the numerical solution of nonlinear and variable coefficient wave equations," *SIAM Rev.*, vol. 15, p. 423, 1972.
- [31] C. Xu, J. Tang, and S. Piao, "Developments of parabolic equation method in the period of 2000–2016," *Chin. Phys. B*, vol. 25, no. 12, pp. 1–12, Dec. 2016, doi: [10.1088/1674-1056/25/12/124315](https://doi.org/10.1088/1674-1056/25/12/124315).
- [32] Q. Guo and Y. L. Long, "Pade second-order parabolic equation modeling for propagation over irregular terrain," *IEEE Antennas Wireless Propag. Lett.*, vol. 16, pp. 2852–2855, 2017, doi: [10.1109/LAWP.2017.2749603](https://doi.org/10.1109/LAWP.2017.2749603).
- [33] *IEEE Standard Definitions of Terms for Radio Wave Propagation*, Standard IEEE 211-1969, (ANSI C16.40-1972), Jan. 1969, pp. 1–8, doi: [10.1109/IEEESTD.1969.7370739](https://doi.org/10.1109/IEEESTD.1969.7370739).
- [34] *IEEE Standard Definitions of Terms for Radio Wave Propagation*, ANSI/IEEE Standard 211-1977, Aug. 1977, pp. 1–15, doi: [10.1109/IEEESTD.1977.120942](https://doi.org/10.1109/IEEESTD.1977.120942).
- [35] *IEEE Standard Definitions of Terms for Radio Wave Propagation*, IEEE Standard 211-1990, Feb. 1991, pp. 1–24, doi: [10.1109/IEEESTD.1991.101057](https://doi.org/10.1109/IEEESTD.1991.101057).
- [36] V. Monebhurrun, "IEEE standard 211-2018: IEEE standard definitions of terms for radio wave propagation [stand on standards]," *IEEE Antennas Propag. Mag.*, vol. 61, no. 3, p. 126, Jun. 2019, doi: [10.1109/MAP.2019.2907906](https://doi.org/10.1109/MAP.2019.2907906).
- [37] G. Feng and J. Huang, "A geometric optics method for calculating light propagation in gravitational fields," *Optik*, vol. 194, Oct. 2019, Art. no. 163082, doi: [10.1016/j.ijleo.2019.163082](https://doi.org/10.1016/j.ijleo.2019.163082).
- [38] R. G. Ligo and O. C. Durumeric, "Conformal transformations and curvature," *J. Knot Theory Ramifications*, vol. 28, no. 2, Feb. 2019, Art. no. 1950020, doi: [10.1142/S0218216519500202](https://doi.org/10.1142/S0218216519500202).
- [39] F. Chambat and B. Valette, "Mean radius, mass, and inertia for reference earth models," *Phys. Earth Planet. Interiors*, vol. 124, nos. 3–4, pp. 237–253, Aug. 2001, doi: [10.1016/S0031-9201\(01\)00200-X](https://doi.org/10.1016/S0031-9201(01)00200-X).
- [40] B. R. Bean and G. D. Thayer, "Models of the atmospheric radio refractive index," *Proc. IRE*, vol. 47, no. 5, pp. 740–755, May 1959, doi: [10.1109/JRPROC.1959.287242](https://doi.org/10.1109/JRPROC.1959.287242).
- [41] Y. Zeng, U. Blahak, M. Neuper, and D. Jerger, "Radar beam tracing methods based on atmospheric refractive index," *J. Atmos. Ocean. Technol.*, vol. 31, no. 12, pp. 2650–2670, Dec. 2014, doi: [10.1175/JTECH-D-13-00152.1](https://doi.org/10.1175/JTECH-D-13-00152.1).

- [42] A. Iqbal and V. Jeoti, "Numerical modeling of radio wave propagation in horizontally inhomogeneous environment using split-step wavelet method," in *Proc. 4th Int. Conf. Intell. Adv. Syst. (ICIAS)*, Kuala Lumpur, Malaysia, Jun. 2012, pp. 200–205, doi: [10.1109/ICIAS.2012.6306187](https://doi.org/10.1109/ICIAS.2012.6306187).
- [43] F. Gauffillet and E. Akmansoy, "Maxwell fish-eye and half-Maxwell fish-eye based on graded photonic crystals," *IEEE Photon. J.*, vol. 10, no. 3, Jun. 2018, Art. no. 4700210, doi: [10.1109/JPHOT.2018.2835157](https://doi.org/10.1109/JPHOT.2018.2835157).
- [44] H. Ohno, "Symplectic ray tracing based on Hamiltonian optics in gradient-index media," *J. Opt. Soc. Amer. A, Opt. Image Sci.*, vol. 37, no. 3, pp. 411–416, Mar. 2020, doi: [10.1364/JOSAA.378829](https://doi.org/10.1364/JOSAA.378829).
- [45] M. R. Forouzzeshfard and T. Tyc, "Photonic crystals composed of Eaton lenses and invisible lenses," *Phys. Rev. A, Gen. Phys.*, vol. 95, no. 1, Jan. 2017, Art. no. 013822, doi: [10.1103/PhysRevA.95.013822](https://doi.org/10.1103/PhysRevA.95.013822).
- [46] A. Bourgoïn, M. Zannoni, and P. Tortora, "Analytical ray-tracing in planetary atmospheres," *Astron. Astrophys.*, vol. 624, no. A41, pp. 1–42, Apr. 2019, doi: [10.1051/0004-6361/201834962](https://doi.org/10.1051/0004-6361/201834962).
- [47] P. Sakic, V. Ballu, W. C. Crawford, and G. Wöppelmann, "Acoustic ray tracing comparisons in the context of geodetic precise off-shore positioning experiments," *Mar. Geodesy*, vol. 41, no. 4, pp. 315–330, Jul. 2018, doi: [10.1080/01490419.2018.1438322](https://doi.org/10.1080/01490419.2018.1438322).
- [48] C.-W. Tseng, Y.-F. Chang, J.-W. Liu, and C.-M. Lin, "A multi-azimuth seismic refraction study for a horizontal transverse isotropic medium: Physical modelling results," *Geophys. Prospecting*, vol. 66, no. 1, pp. 13–25, Jan. 2018, doi: [10.1111/1365-2478.12526](https://doi.org/10.1111/1365-2478.12526).
- [49] T. Dabrowski, W. C. Barott, and B. Himed, "Effect of propagation model fidelity on passive radar performance predictions," in *Proc. IEEE Radar Conf. (RadarCon)*, Arlington, VA, USA, May 2015, pp. 1503–1508, doi: [10.1109/RADAR.2015.7131234](https://doi.org/10.1109/RADAR.2015.7131234).
- [50] G. Feng, J. Huang, and M. Yi, "Composite refractive index on electromagnetic wave propagating in spherical medium," *IEEE Trans. Antennas Propag.*, vol. 68, no. 3, pp. 2297–2303, Mar. 2020, doi: [10.1109/TAP.2019.2948496](https://doi.org/10.1109/TAP.2019.2948496).



GUOXU FENG received the bachelor's, master's, and Ph.D. degrees from Beihang University (BUAA), in 2008, 2011, and 2020, respectively.

He was engaged in stealth design of aircraft with CASIC, from 2011 to 2014. His current research interests include composite structure design, low observability technology, combat effectiveness, wave propagation, antenna modeling, clutter modeling, target signal detection, theory of relativity, and quantum mechanics.



JUN HUANG received the M.S. and Ph.D. degrees in aircraft design from the School of Aeronautic Science and Engineering, Beihang University (BUAA), Beijing, China, in 1997 and 2000, respectively.

He is currently a Professor with BUAA. His research interests include aircraft design, effectiveness analysis, and stealth technology.



MINGXU YI was a Postdoctoral Researcher with Beihang University, China, from 2013 to 2016. He is currently an Assistant Professor with the School of Aeronautic Science and Engineering, Beihang University. His research interests include rotor aerodynamic noise calculation and RCS reduction technology.

...